Chemical Engineering Journal 144 (2008) 312–316

Contents lists available at ScienceDirect

Chemical Engineering Journal

journal homepage: www.elsevier.com/locate/cej

Excitational metamorphosis of surface flowfield under an impinging annular jet

Václav Tesař*, Zdeněk Trávníček

Institute of Thermomechanics of the Academy of Sciences of the Czech Republic, v.v.i., Dolejskova 5, 182 00 Prague, Czech Republic

ARTICLE INFO

Article history:
Received 3 March 2008
Received in revised form 11 June 2008
Accepted 28 June 2008

Keywords:
Flow topology
Impinging jets
Annular jets
Stagnation points
Heat and mass transfer

ABSTRACT

In the course of development of controlled impinging jets, a phenomenon was discovered that may seem to be rather strange at first sight. It is a change of topology – in fact, in the central region, the very reversal of topological character – of the surface flows occurring when oscillation is superimposed on the supply flow into an annular nozzle generating the impinging jet. The change, apart from its interesting hydrodynamic aspects, is of importance for heat and mass transfer applications as it promises a considerable increase of total transfer rate as well as an increase of the area covered by the impingement.

1. Introduction

Impinging jets are widely used in chemical and process engineering, especially for providing heat and mass transfer between a fluid and a solid surface. Their advantage is the capability to achieve the highest transfer rates among all flowfield alternatives—see, e.g. [1–3], and [4]. Increasingly often in recent time, questions arise about a possibility of controllability of the impinging flow [5]. Economy and effectiveness call for replacing the so far used passive, invariable impingement flows by a version making possible modulation or variation of the flowfield in response to some signal derived from sensed changes in the conditions on the heated (or cooled) object. As an example, a feedback control system may adjust the transfer intensities under individual nozzles of a multi-nozzle system [1,6] so as to remove any excessive local deviations in the surface conditions. It may be desirable to ensure this way an evenness of the heating or mass transfer action over the surface. Conversely, in other cases the control action may be used to produce a required local extreme.

The modulation may be ensured by mechanical means—motions or re-arrangements of nozzle components. This, however, is in general not the desirable solution as the mechanisms and their drives tend to be expensive and in the long run unreliable. A more promising solution is currently found in designs that change the impingement flowfield by using its response to oscillation or acoustic excitation of the flow supplied into the nozzle. This may even achieve some heat (or mass) transfer enhancement. Possibilities of the acoustic control, mainly from the point of view of the enhancement, were investigated, e.g. by Liu and Sullivan [7], Gau et al. [8], Hwang and Cho [9], Trávníček and Tesař [10], and O'Donovan and Murray [11]. A particularly attractive solution is generation of the oscillations by no-moving-part self-excited fluidic oscillators, for example of the types described in Refs. [12–15]. Apart from their robust set-up, which makes them immune to external effects such as, e.g. shocks or temperature changes, their inexpensive manufacturing, and no need of maintenance, they have the advantage of using for generation of the oscillation just a small part of the pressure energy of the supplied fluid. They do not require external energy supply (such as, e.g., bringing in electricity by electric conductors into motors driving a mechanically modulated nozzle).

Considering the relatively very small applied excitation power, some of the impinging jet configurations can respond by very substantial change in the overall character of the jet flowfield. In particular, in annular impinging jets the relatively weak superimposed oscillation can change the very basic topology of fluid flows on the impingement surface. The basic "centrifugal" surface flowfield according to Fig. 1, with fluid moving away from the central stagnation point, was demonstrated to undergo a metamorphosis (defined in the dictionary as "*a striking change in appearance or character*") into the "centripetal" flow, directed towards the central stagnation point, Fig. 2. The fluid in this case is brought towards the surface by the motion in the vicinity of the stagnation circle surrounding the central region.

* Corresponding author. Tel. +420 2 6605 2270.
E-mail address: tesar@it.cas.cz (V. Tesař).

1385-8947/$ – see front matter © 2008 Elsevier B.V. All rights reserved.
doi:10.1016/j.cej.2008.06.036

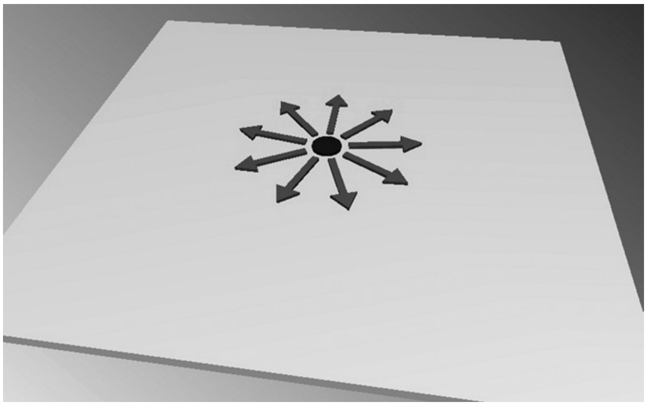

Fig. 1. Character of the standard flow on the impingement surface. Fluid moves away from the central source-type stagnation point.

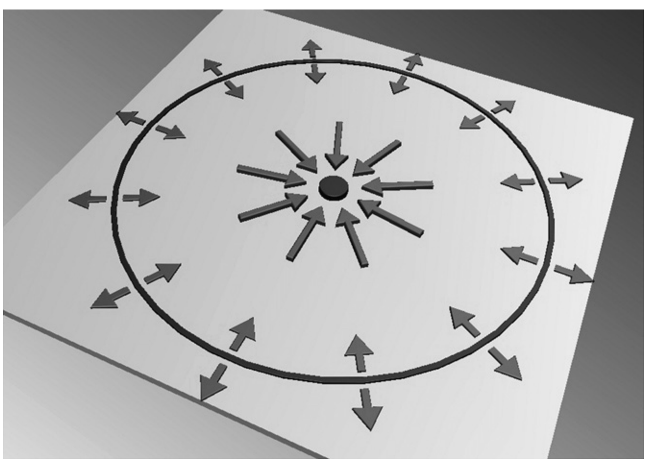

Fig. 2. Transformed flow on the surface, as caused by the applied pulsation. Fluid flows towards the central sink-type stagnation point from the surrounding stagnation circle.

2. Annular impinging jets

The existence of two different topological characters of the surface flowfield under the impinging annular jet, Fig. 3, is not a new feature—but the transition between them has been so far known only as being caused by a change in the distance h from the nozzle

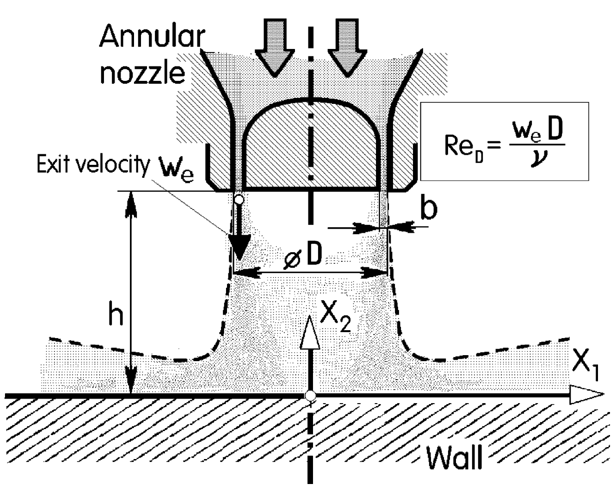

Fig. 3. Annular impinging jet and its main parameters.

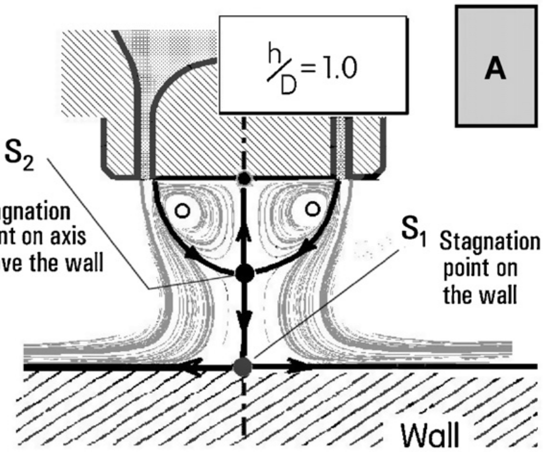

Fig. 4. Character of the flow of an annular jet impinging on a sufficiently distant flat wall. Computed pathlines of the flowfield show the stationary vortex ring remaining attached under the nozzle.

to the wall [16,17,19]. In both flowfield configurations, the dominant factor is the presence of a stationary vortex ring attached to the nozzle. The “centrifugal” flowfield is found if the impingement wall is positioned so far from the nozzle – Fig. 4 – that the vortex ring region is closed at the stagnation point S_2 on the nozzle axis above the surface. The closure is caused by the entrainment into the jet. This removes fluid from the vortex ring region and generates there a low pressure that bends the initially straight jet flow towards the axis.

The change into the “centripetal” configuration, as shown in Fig. 5, is achieved by moving the impingement wall towards the nozzle. This existence of the two topologies and the transition between them is supported not only by experimental data [19], but was confirmed also by extensive computational flowfield solutions, the results of which – in the form of computed pathlines – is presented in Figs. 4 and 5. The solved equation is the standard Reynolds-averaged Navier–Stokes equations with modelled turbulent gradient transport term. The geometry of the computational domain agreed exactly with the laboratory model used in experiments described below. The computations were performed with FLUENT finite volume solver using unstructured grids. The model of turbulence was standard two-equation model as provided by software provider (using standard set of turbulence model constants). The low Reynolds number behaviour of turbulence was modelled using the RNG approach, again as provided. The number of grid

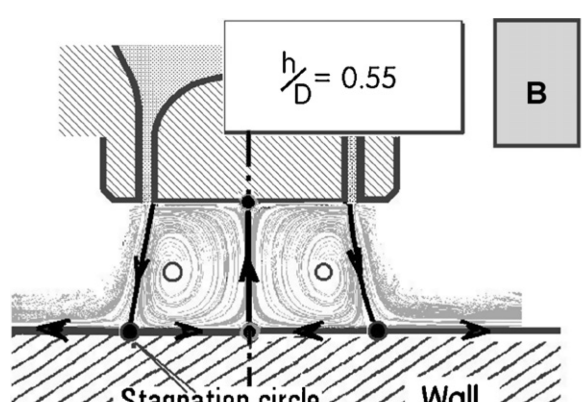

Fig. 5. In steady states, the ring vortex region may reach up to the wall – forming there the pattern according to Fig. 2 – only if the wall is placed nearer to the nozzle.

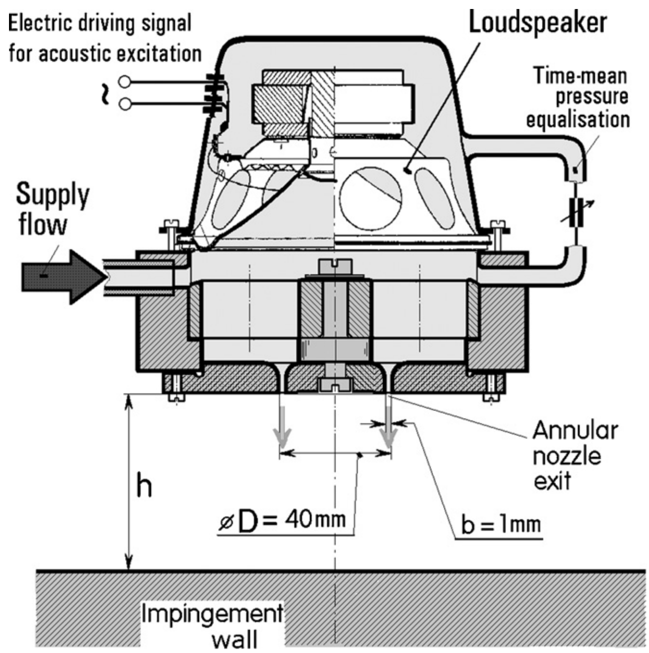

Fig. 6. The model annular nozzle with acoustic excitation used in the laboratory investigations.

elements was of the order 10^4, the actual values varied due to the gradual grid refinements in the regions of high local gradient of velocity magnitude.

3. Laboratory test model

In spite of the intention to generate in the final version the pulsation by fluidic oscillators [12,15], it was considered more convenient for the laboratory tests to use an electromechanical actuator. One of the reasons for this choice is the considerable effort needed at this stage of their development to design and develop a high-performance fluidic oscillator. Another was the inconvenient property of no-moving-part self-excited oscillators to vary their oscillation frequency with the flow rate.

The essential component of the actuator was a low-frequency electrodynamic loudspeaker, of nominal membrane diameter 100 mm, Fig. 6. This size, together with the requirement of sufficient amplitude of the generated pulsation, resulted in the relatively small size of the nozzle exit. As shown in Figs. 6 and 7, the exit slot width was only 1 mm and the outer diameter D = 40 mm. This annular geometry was made by placing a 38 mm diameter round central insert into the 40 mm nozzle. The insert was held in its position by five radial arms remaining in the nozzle body after drilling in it five large holes, Fig. 8.

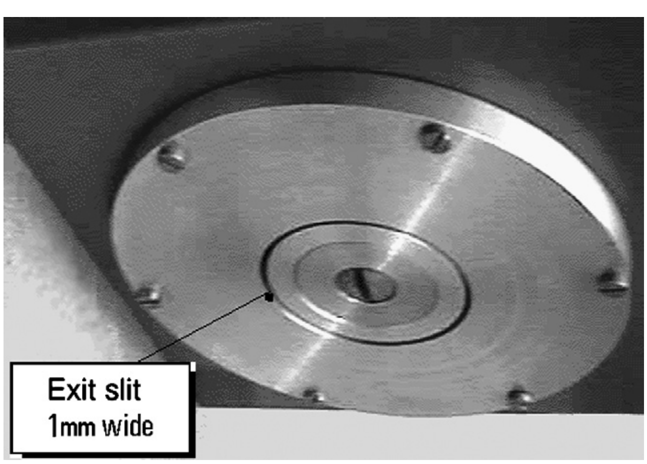

Fig. 7. View of the nozzle model from below, showing the central body delimiting the exit slit.

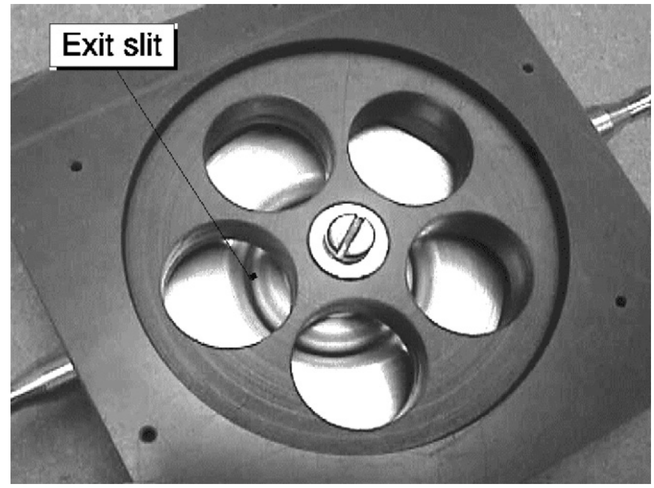

Fig. 8. Internal layout of the model nozzle. The central insert, held by the 5 radial arms, fills the exit of the 40 mm circular nozzle leaving on its periphery only the 1 mm wide exit slit.

The response to excitation by the loudspeaker was frequency dependent due to resonance in the cavity upstream from the exit slit. Recent tests with analogous configuration, [20], have shown that the resonant conditions are negligibly influenced by compressibility of the air in the cavity. The decisive factor is the compliance of the membrane of the loudspeaker. In the present case, the response was evaluated in a preliminary test, the results of which are shown in Fig. 9. It is evident that most effective driving was obtained at one of the two resonant peak frequencies, either at f_{res1} = 263 Hz or the somewhat weaker f_{res2} = 692 Hz.

4. Experiments and evidence

The tests were made with air as the working fluid, using the single ratio of the nozzle diameter to gap width. This ratio was 40. The tests were made at a single Reynolds number Re_D = 41,800. The methods used for the investigations were hot wire anemometry, quantitative naphthalene sublimation measurements (Fig. 10), and smoke wire visualisation (Fig. 11). Also used in a supporting

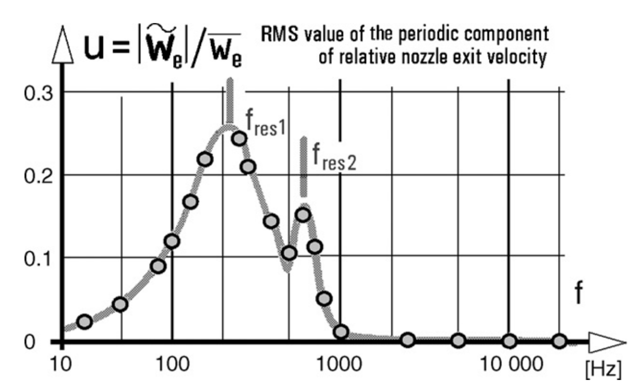

Fig. 9. Acoustic resonance properties of the nozzle cavity, evaluated by measuring the velocity amplitude in the exit while the electric driving power was kept constant. The subsequent mass transfer tests focused on excitation at the two resonant frequencies.

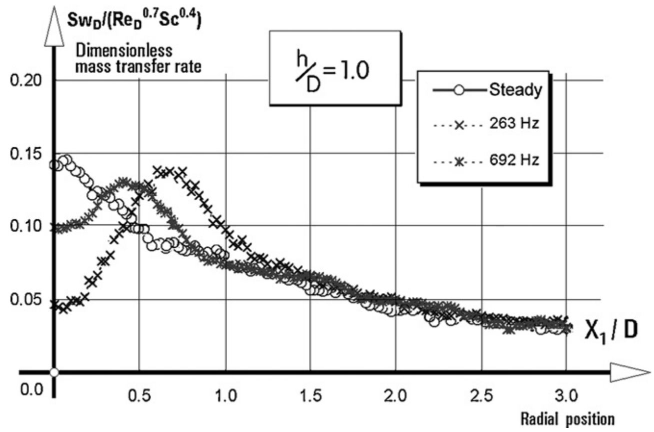

Fig. 10. Results, presented in terms of the radial distribution (along the radius X_1, Fig. 3) of the Sherwood number *Sw*, of naphthalene sublimation method measurements of mass transfer from the surface.

role, to provide an idea about the overall character of the flowfield, were numerical flowfield computations. These were analogous to the steady flow solutions described in association with Figs. 4 and 5 but were performed as time dependent, with harmonic inlet fluid motion superimposed on the steady inlet flow component and converged at 20 time steps over each oscillation period.

The smoke wire technique used a thin wire exposed into the flow, coated at the beginning of each test with paraffin oil and heated by the Joule effect of a direct electric current—as described, e.g., by Trávníček and Tesař [10].

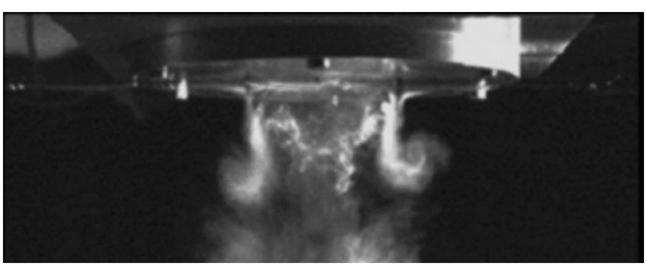

Fig. 11. The outer ring vortex generated in the excited jet visualised by the smoke wire method.

The local mass transfer was measured using the naphthalene sublimation method, an exhaustive description of which is provided by Goldstein and Cho [18]. The local mass transfer coefficient is calculated from the measured sublimation depth Δy as

$$h_m = \frac{\rho_n R_n T_w}{P_{sat}} \frac{\Delta y}{\Delta t} \quad (1)$$

where ρ_n is the density of solid naphthalene, R_n is the naphthalene gas constant, T_w is the surface temperature, P_{sat} is the saturated vapor pressure of naphthalene at T_w, and Δt is the run duration. The non-dimensional expression of the mass transfer coefficient is the Sherwood number,

$$Sw_D = \frac{h_m D}{\chi_n} \quad (2)$$

where χ_n is the mass diffusion coefficient of naphthalene vapor in air, calculated for the measured temperature and pressure [18]. A more detailed description of this experimental method and its uncertainties was described by Trávníček and Tesař [10].

All these methods have shown that the original steady-state centrifugal pattern of Figs. 1 and 4, obtained when the nozzle was placed at the distance $h = D = 40$ mm, is transformed by the action of pulsation into the centripetal pattern of Fig. 2.

The unequivocal evidence is presented in Fig. 10, displaying (in non-dimensionalised presentation) the measured distribution of local intensities of the naphthalene removal from the surface. The source-type stagnation objects on the surface are characterised by the local maxima of the transport intensity while the sink-type stagnation point is characterised by a minimum. Obviously, as expected, the distribution curve shape for steady flow corresponding to Fig. 1 has just the local maximum on the centreline (at left in Fig. 10), the intensity decreasing monotonously along the radius X_1 (Fig. 3). The application of the excitation changes this pattern into the one from Fig. 2. There is a sink point minimum on the axis and a local source maximum away from the axis—the latter, due to the axial symmetry, has to form the stagnation circle.

It is less easy to deduce the mechanism of this change. Initially, the present authors were inclined to believe that the region occupied by the stationary vortex ring is extended by the excitation towards the surface so that the flowfield would be topologically equivalent to the one shown in Fig. 5. However, more recent time-dependent computation results, of which Fig. 12 presents an example computed at a particular instant of time in the settled

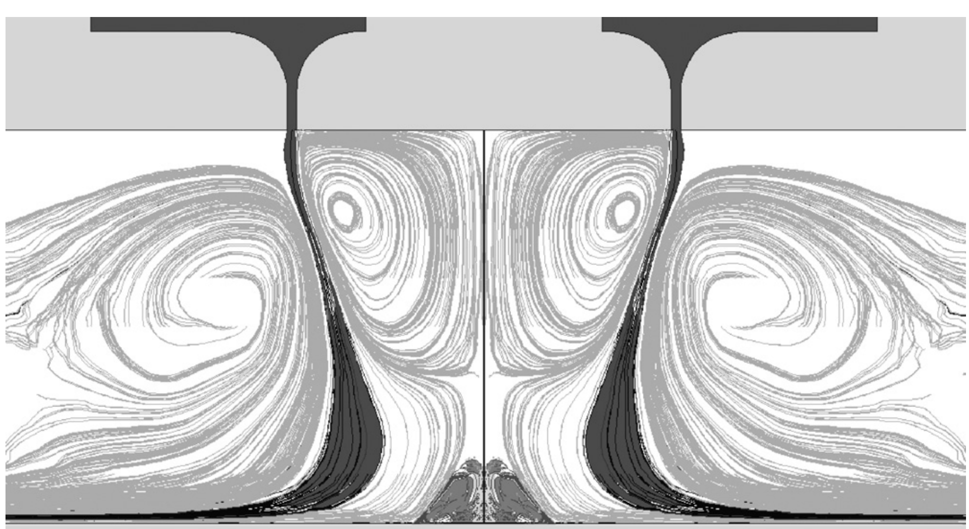

Fig. 12. En example of computed time-mean pathlines in the excited jet reveals the presence of a small standing vortex in the central impingement region.

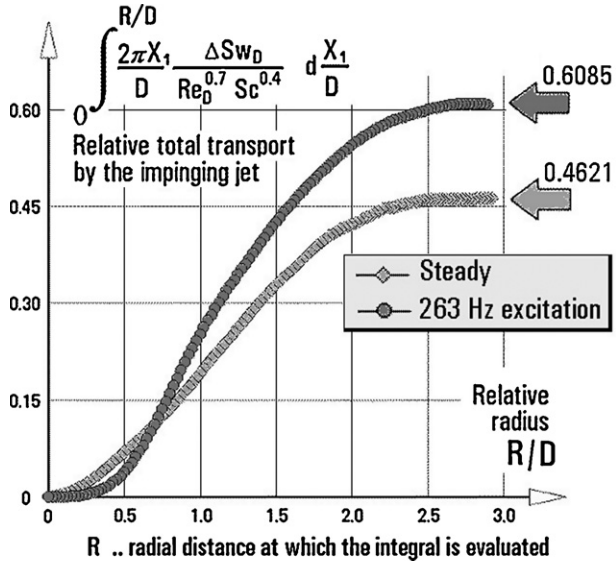

Fig. 13. Integrated total mass transport from the wall under the annular jet evaluated for the two curves (one for steady state, the other for excitation at the resonant frequency f_{res1}, Fig. 9) presented in Fig.10.

conditions (i.e. after several periods) suggest a different picture. Instead of the expected elongation of the top vortex ring towards the wall the computational results suggest a formation of another, small vortex ring surrounding the wall stagnation point. Smoke visualisation attempts, while revealing quite well the conditions near the nozzle, Fig. 11, unfortunately failed to provide an unequivocal answer as to what happens near the wall, since the smoke there is too much mixed with the surrounding fluid.

Even though the present investigations were aimed primarily at understanding the hydrodynamics of the excited annular impinging jets and the remarkable change of the topology of the surface flow, an integration of the experimentally obtained local mass transfer intensities – as shown in Fig. 13 – shows a significant increase in the total transport. The increase is by as much as 32%. While this result of a single experiment cannot form a basis for any definite conclusions, the unequivocal demonstration of the increase makes this of considerable importance for designers of heat and/or mass transfer equipment. It would be useful as a way towards a further increase of the effectiveness of the impinging jet flows, known to offer the highest transfer effectiveness and used in situations where extreme values are required. Recently, another support for the improvement obtained by flow oscillation in annular impinging flows was found in different experiments described in [13].

5. Conclusions

Application of pulsation to the fluid flow supplied to an annular nozzle and impinging upon an opposing flat wall was demonstrated to change completely the surface flow patterns. The tests were so far made with a single geometry, having nozzle diameter to gap width ratio 40 and the nozzle placed at $h = D$ from the wall, at a single Reynolds number $Re_D = 41\,800$. The pulsation was applied to the settling chamber upstream from the nozzle exit. The chamber resonance determined the excitation frequencies to be in the acoustic range. Initially, the change was believed to be a transition from the pattern A in Fig. 4 to the pattern B in Fig. 5, i.e. an elongation of the stationary vortex ring region towards the impingement wall. However, more recent experience suggests the change may involve development of a more complex topology. The transition was studied as an interesting hydrodynamic problem, but the demonstrated associated increase of transfer rate – in a flow that is the one already reaching the maximum of what can be done in heat and mass transfer – suggests that the phenomenon might be of direct practical importance in chemical and process engineering.

Acknowledgments

Support of Grant Agency of the Czech Republic by grant no. 101/07/1499, of Grant Agency of the Academy of Sciences of the Czech Republic by grant no. IAA200760705 and by the research plan AV0Z20760514.

References

[1] H. Martin, Heat and mass transfer between impinging gas jets and solid surfaces, Adv. Heat Transfer 13 (1977) 1–60.
[2] B.W. Webb, C.-F. Ma, Single-phase liquid jet impingement heat transfer, Adv. Heat Transfer 26 (1995) 105–217.
[3] S.V. Garimella, Heat transfer and flow fields in confined jet impingement, Annu. Rev. Heat Transfer XI 413 (2000) 413–494.
[4] S.J. Downs, E.H. James, Jet impingement heat transfer—a literature survey, in: Proceedings of the National Heat Transfer Conference, ASME, Pennsylvania, PA, 1987, 87-HT-35.
[5] V. Tesař, Pressure-Driven Microfluidics, Artech House Publishers, Boston/London, 2007.
[6] B.P. Whelan, A.J. Robinson, Effect of nozzle geometry on pressure drop and heat transfer to both free-surface and submerged liquid jet arrays, in: Proceedings of the 5th European Thermal-Sciences Conference, Eindhoven, FCV 3, 2008.
[7] T. Liu, J.P. Sullivan, Heat transfer and flow structures in an excited circular impinging jet, Int. J. Heat Mass Transfer 39 (17) (1996) 3695–3706.
[8] C. Gau, W.Y. Sheu, C.H. Shen, Impingement cooling flow and heat transfer under acoustic excitations, Trans. ASME J. Heat Transfer 119 (4) (1997) 810–817.
[9] S.D. Hwang, H.H. Cho, Effects of acoustic excitation positions on heat transfer and flow in axisymmetric impinging jet: main jet excitation and shear layer excitation, Int. J. Heat Fluid Flow 24 (2) (2003) 199–209.
[10] Z. Trávníček, V. Tesař, An annular impinging jet with recirculation zone expanded by acoustic excitation, Int. J. Heat Mass Transfer 47 (10) (2004) 2329–2341.
[11] T.S. O'Donovan, D.B. Murray, Heat transfer to an acoustically excited impinging air jet, in: Proceedings of the 5th European Thermal-Sciences Conference, Eindhoven, JET 6, 2008.
[12] V. Tesař, C.-H. Hung, W. Zimmerman, No-moving-part hybrid-synthetic jet actuator, Sensors and Actuators A 125 (2) (2006) 159–169.
[13] V. Tesař, Conditions on the wall under a pair of phase-shifted, impinging hybrid-synthetic annular jets, in: Paper ISFV12-86.1, Proceedings of the 12th International Symposium on Flow Visualization, Göttingen, September, 2006.
[14] V. Tesař, Z. Trávníček, J. Kordík, Z. Randa, Experimental investigation of a fluidic actuator generating hybrid-synthetic jets, Sensors and Actuators A 138 (July) (2007) 213–220.
[15] V. Tesař, Configurations of fluidic actuators for generating hybrid-synthetic jets, Sensors and Actuators A: Physical 138 (August (2)) (2007) 394–403.
[16] Y. Kokoshima, A. Shimizu, T. Murao, Numerical analysis of annular turbulent jet impinging on flat plate, in: Proceedings of the Symp. FLUCOME'91, San Francisco, 1991, p. 205.
[17] V. Tesař, Z. Trávníček, Review: Increasing heat and/or mass transfer rates in impinging jets, Journal of Visualization 8 (2) (2005) 91–98.
[18] R.J. Goldstein, H.H. Cho, A review of mass transfer measurements using naphthalene sublimation, Experimental Thermal and Fluid Science 10 (1999) 416–434.
[19] V. Tesař, M. Jílek, Z. Randa, Topology changes in an annular impinging jet flow, in: Proceedings of the Colloq. "Topical Problems of Fluid Mechanics 2001", Inst. of Thermomechanics AS CR Prague, Prague, Czech Republic, 2001, ISBN 80-85918-62-5, p. 121.
[20] P. Krejčí, Z. Trávníček, V. Tesař, J. Kordík, M. Pavelka, Frequency characteristics of an annular synthetic jet actuator of large inner diameter, in: Proceedings of the Conference 'Experimental Fluid Mechanics 2007', Liberec, Czech Republic, November, 2007.